

Infrared absorption spectrum of matrix-isolated noble-gas hydride molecules: Fingerprints of specific interactions and hindered rotation

Leonid Khriachtchev,^{a)} Antti Lignell, Jonas Juselius, and Markku Räsänen
Department of Chemistry, University of Helsinki, P.O. Box 55, FIN-00014 Helsinki, Finland

Elena Savchenko
Verkin Institute for Low Temperature Physics and Engineering, Kharkov 61103, Ukraine

(Received 28 September 2004; accepted 11 October 2004; published online 15 December 2004)

Noble-gas hydride molecules with the general formula HNgY (Ng denotes noble-gas atom and Y denotes electronegative fragment) are usually prepared in solid noble gases. In many cases, the matrix-isolated HNgY molecules show a characteristic structure of the H–Ng stretching absorption: A close doublet as the main spectral feature and a weaker satellite at higher energy. This characteristic band structure is studied here for matrix-isolated HXeBr and HKrCl molecules. Based on the experimental and theoretical results, we suggest a model explaining the common features of the band structure of the HNgY molecules in noble-gas matrices. In this model, the main doublet bands are attributed to matrix sites where the splitting is caused by specific interactions of the embedded molecule with noble-gas matrix atoms in certain local morphology. The weaker blueshifted band is probably a fingerprint of hindered rotation (libration) of the embedded molecule in the lattice. This librational band has a mirror counterpart at lower energies appearing at higher matrix temperatures. Our present *ab initio* calculations for the one-to-one Xe··HXeBr complexes and the simulation of hindered rotation in a matrix support this image. © 2005 American Institute of Physics. [DOI: 10.1063/1.1827592]

I. INTRODUCTION

Hydrogen-containing noble-gas molecules with the general formula HNgY (Ng denotes noble-gas atom and Y denotes electronegative fragment) were first reported in 1995.^{1,2} Twenty molecules of this family have been synthesized and characterized to date. The first identified species were HXeCl, HXeBr, HXeI, and HKrCl,¹ and the recent examples are an argon compound HArF,^{3–5} a noble-gas open-shell species HXeO,⁶ and organo-noble-gas insertion molecules prepared from acetylene and diacetylene.^{7–10} The developed preparation procedure combines UV photolysis of HY precursors in a low-temperature noble-gas matrix and thermal mobilization of the photogenerated hydrogen atoms.² Most of the relevant studies have been performed in noble-gas matrices, however, some of these HNgY molecules were reported to be prepared in noble-gas clusters in the gas phase.^{11,12}

The matrix-isolated HNgY molecules are easily detectable via the strong infrared (IR) absorption of the H–Ng stretching mode.^{1–10} It was noticed from the beginning that this absorption possesses a complicated band structure. In many cases (HXeI, HXeBr, HXeCN, HXeSH, HKrCN, HKrCl),^{1,2,13,14} the structured band shows a characteristic shape: a close doublet and a relatively weak higher energy band, and no detailed interpretation of this structure has been suggested. Most probably, this structure originates from properly isolated HNgY molecules, i.e., complexation with contaminants can be neglected. In this situation, the observed

band structure is attributable to interactions of the embedded molecule with the noble-gas host atoms.

Somewhat different shapes of the H–Ng stretching absorption bands have also been observed. A number of molecules (HXeCCXeH, HKrCCH, HXeC₄H) show a more extensive H–Ng stretching band structure, which has been tentatively explained by the matrix-site effect.^{8,10} For matrix-isolated HArF and HKrF, the H–Ng stretching mode exhibits thermally unstable and stable components.^{4,5,15} The suggested experimental interpretation is based on thermal modification of matrix surrounding,^{4,5} and some theoretical studies of this phenomenon are known.^{16–18} For example, Jolkkonen *et al.* connected the 50 cm^{–1} blueshift of the stable band of HArF to a specific interaction of HArF (from the H end) with one Ar matrix atom.¹⁷ As another relevant example, Feldman and Sukhov demonstrated different thermal stability of the 1181 and 1166 cm^{–1} bands of HXeH.¹⁹ Blueshifts of the bands from their monomer positions can also be caused by complexation with impurities as it was demonstrated for the HXeOH–water complex,²⁰ and for complexes of HArF, HKrF, and HKrCl with nitrogen.²¹

In the present work, we investigate the characteristic IR absorption band structure of matrix-isolated HXeBr and HKrCl. Based on the experimental and theoretical results, we suggest a model explaining the common features of the band structure of the HNgY molecules. The doublet of the main spectral feature is described as matrix sites due to specific interactions with noble-gas atoms in well-defined local matrix morphologies. The weaker higher-energy band is supposed to originate from hindered rotation of HNgY in the matrix environment.

^{a)}Electronic mail: Leonid.Khriachtchev@Helsinki.Fi

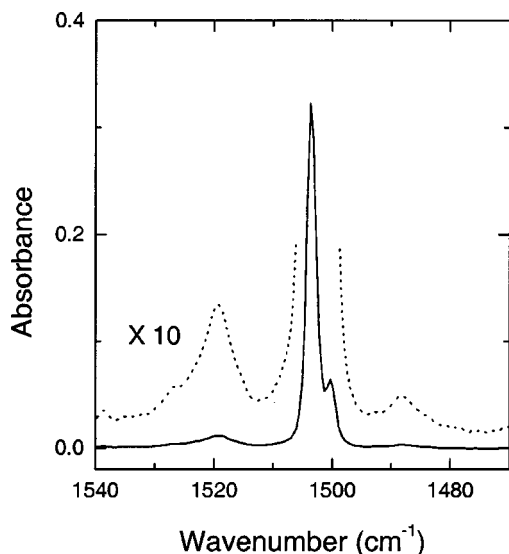


FIG. 1. IR absorption spectrum of matrix-isolated HXeBr in the H–Xe stretching region. The photolyzed HBr/Xe (1:1000) sample was annealed at 35 K for 155 min. The deposition temperature was 30 K. The spectrum was measured at 8 K.

II. EXPERIMENTAL DETAILS AND RESULTS

The procedures used here are typical for experiments with HNgY molecules in noble-gas matrices.² The HY gas mixture (HY = HBr or HCl) with a noble gas (Ng = Xe or Kr) is prepared in a certain proportion ($\leq 1:1000$) and then deposited onto a cold CsI window in a closed-cycle helium cryostat (APD, DE 202A). The obtained matrices are quite monomeric with respect to HY as judged by the IR absorption spectra. The HY precursor is photolyzed with an eximer laser (MPB, MSX-250) operating at 193 nm. Annealing of the photolyzed matrices mobilizes the photogenerated H atoms, which leads to the formation of HNgY molecules. The IR absorption spectra are recorded with a Nicolet 60 SX FTIR spectrometer using a resolution of 1 cm^{-1} .

A typical spectrum of HXeBr monomer in a Xe matrix is presented in Fig. 1 for the H–Xe stretching region. The components of the main spectral feature are at 1503.7 and 1500.2 cm^{-1} at 8 K, and the weaker higher-energy band is at 1519.6 cm^{-1} . First, we study this spectrum as a function of the annealing time and annealing temperature. Figure 2(a) compares the spectra measured at 8 K after annealing at 35 K for 5 min (the lower trace, notice the multiplication factor) and for 155 min (the upper trace). The intensity ratio of the doublet components (bands S_1 and S_2 in our notation, see Fig. 2) clearly differs for these two spectra. This intensity ratio as a function of the annealing time (35 K) is shown in Fig. 2(b), and the dotted horizontal line gives the value after additional annealing at 45 K for 5 min. The band intensities were obtained by fitting the spectra by Lorentzian curves. The S_2/S_1 intensity ratios measured after 5 min annealing at 35 K and 45 K differ in this experiment by a factor of ~ 5 . In contrast, the $L_1/(S_2+S_1)$ intensity ratio changes insignificantly.

Next, the IR absorption spectrum of HXeBr is studied as a function of the matrix temperature. Figure 3 presents the H–Xe stretching absorption band measured at 10, 30, and 50 K. The main band shifts to lower energies and broadens with

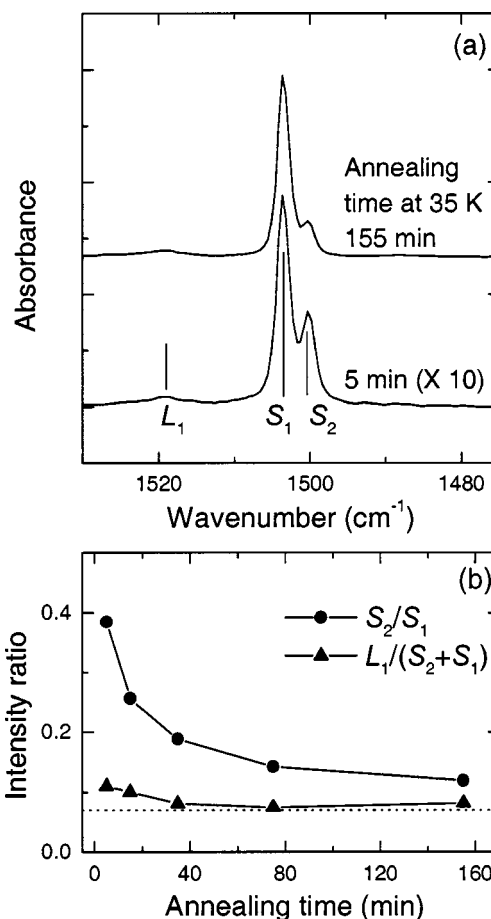


FIG. 2. (a) H–Xe stretching absorption of HXeBr in a Xe matrix for different periods of annealing at 35 K. The deposition temperature was 30 K. The spectra were measured at 8 K. Notice the multiplication factor in the lower trace. (b) The intensity ratios of the bands as a function of the time of annealing at 35 K. The bands are denoted in plot (a). The dotted line gives the S_2/S_1 intensity ratio obtained after additional annealing at 45 K for 5 min.

the increasing temperature, and the two components S_2 and S_1 are still distinguishable with a similar intensity ratio. More importantly for the present study, the lower-energy satellite L_2 at about 1487 cm^{-1} increases at higher temperatures. Actually, this satellite is visible even in the spectrum measured at 8 K (see Fig. 1), and it undoubtedly originates from HXeBr. The temperature dependence of band L_2 is completely reversible, i.e., its intensity decreases at lower temperatures after the rise at higher temperatures. The interval between this band and the main spectral feature is practically equal to the shift of the higher energy peak ($\sim 15 \text{ cm}^{-1}$). The L_2/L_1 intensity ratio as a function of the matrix temperature is shown by triangles in Fig. 4.

The deposition temperature has a noticeable effect on the studied spectra. The spectra presented in Fig. 2 correspond to a deposition temperature of 30 K, which seems to be optimal to resolve the S_1 – S_2 doublet. Deposition at lower temperatures leads to broadening of the bands of the main spectral feature. For deposition at 10–25 K, the S_1 – S_2 doublet is not resolved after annealing at 35 K. However, for deposition at 25 K, the annealing at 60 K produces the well-resolved doublet when the spectrum is measured at 8 K (see Fig. 5).

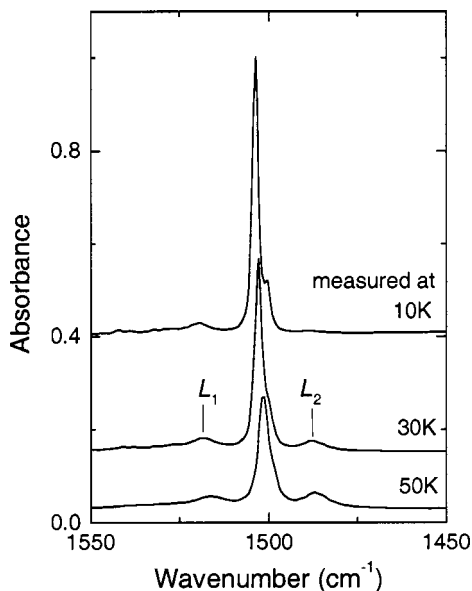


FIG. 3. H–Xe stretching absorption of HXeBr measured at different temperatures. The deposition temperature was 25 K. The photolyzed HBr/Xe (1:1000) sample was annealed at 45 K. The spectral feature rising at higher measurement temperatures is marked as L_2 .

Independent of the deposition temperature, the $L_1/(S_1 + S_2)$ intensity ratio remains practically unchanged (~ 0.08 as measured at 8 K). It should be mentioned here that annealing at temperatures above 45 K promotes additional bands at higher energies from the main spectral feature as seen in Fig. 5. Most probably, they originate from complexes of HXeBr with some matrix species, in analogy with other HNgY molecules,^{20,21} and these additional spectral features are not considered in the present work.

Figure 6(a) presents the H–Kr stretching band of HKrCl in solid Kr. In this experiment we used a very high dilution

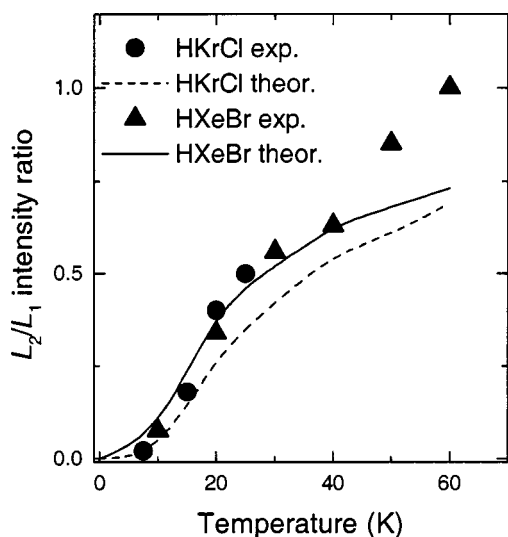


FIG. 4. Intensity ratio of satellites L_2 and L_1 as a function of the matrix temperature (for notations see Fig. 3). Shown are the data for HXeBr and HKrCl. The deposition temperature was 25 K for the HBr/Xe (1:1000) sample and 20 K for the HCl/Kr (1:15000) sample. The symbols represent the experimental data and the lines are from our simulation of hindered rotation.

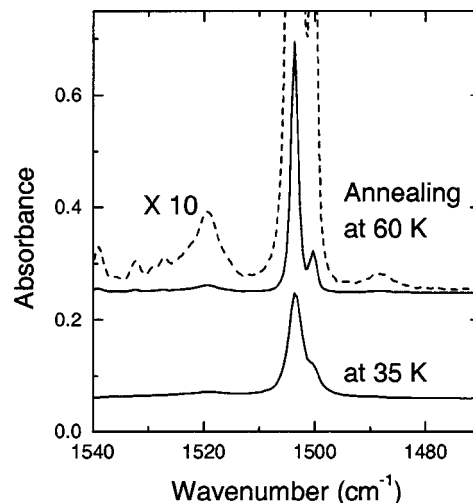


FIG. 5. H–Xe stretching absorption of HXeBr for different annealing temperatures. The deposition temperature was 25 K. The photolyzed HBr/Xe (1:1000) sample was annealed at 35 K for 155 min (the lower trace) and the same sample was annealed at 60 K for 5 min (the upper trace). The spectra were measured at 8 K.

(HCl/Kr $\sim 1/15000$) in order to avoid HCl multimerization, which explains the relatively small intensity of the HKrCl band. It is seen that the shape of the spectrum is qualitatively similar to the spectrum of HXeBr discussed earlier. The main

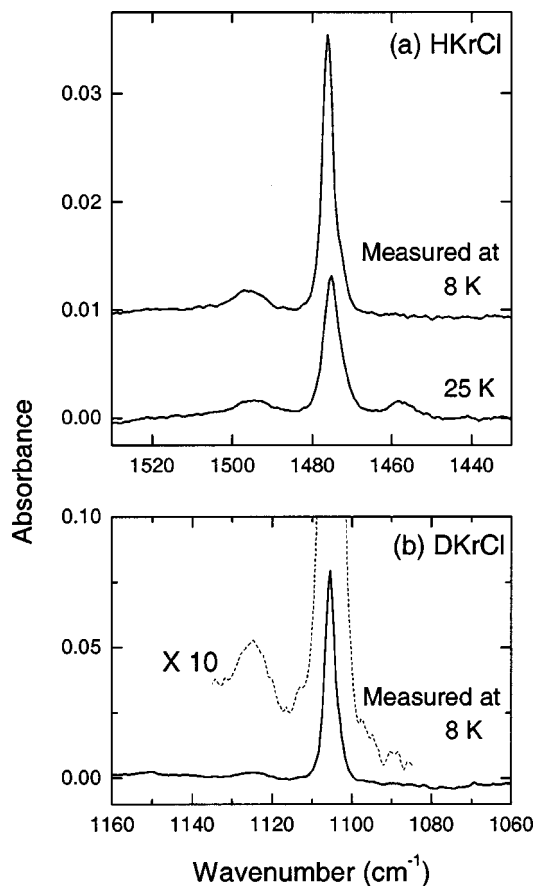


FIG. 6. (a) H–Kr stretching absorption of HKrCl measured at different temperatures. (b) D–Kr stretching absorption of DKrCl measured at 8 K. The magnified spectrum reveals the higher-energy component L_1 . The deposition temperature was 20 K. After 193 nm photolysis, the samples were annealed at 30 K. The data for the deuterated sample is from Ref. 30.

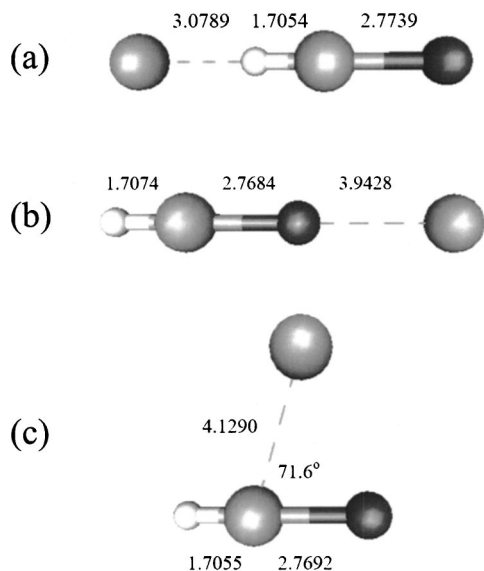


FIG. 7. Three optimized *ab initio* structures of the $\text{Xe}\cdots\text{HXeBr}$ complex. The distances are in angstroms.

spectral feature of HKrCl at $\sim 1476\text{ cm}^{-1}$ clearly exhibits a shoulder at lower energy corresponding to band S_2 . The higher-energy satellite L_1 at $\sim 1496\text{ cm}^{-1}$ is also quite visible. When measured at higher temperatures, the lower-energy satellite L_2 at $\sim 1456\text{ cm}^{-1}$ rises. The L_2/L_1 intensity ratio as a function of the measurement temperature is shown by circles in Fig. 4. Similar to HXeBr , the effect of temperature on the L_2/L_1 intensity ratio is reversible. In the experiment with a deuterated sample, the IR absorption spectrum of DKrCl shows a higher-energy satellite L_1 separated from the main spectral feature by $\sim 20\text{ cm}^{-1}$ [see Fig. 5(b)].

III. THEORETICAL RESULTS

A. *Ab initio* calculations

In this section, we investigate computationally one-to-one interaction between HXeBr and a Xe atom. The quantum chemical *ab initio* calculations on the $\text{Xe}\cdots\text{HXeBr}$ complex were carried out with the GAUSSIAN03 package of computer codes.²² The electron correlation method was the second order Møller-Plesset perturbation theory. The standard split valence basis set 6-311++G(2d,2p) was used to describe H and Br atoms and LaJohn effective core potential was employed for Xe atoms. The interaction energy is found as a difference between energies of the $\text{Xe}\cdots\text{HXeBr}$ complex and the HXeBr and Xe monomers. The interaction energy takes into account the counterpoise basis set error correction and the vibrational zero-point energy. Similar computational approaches have been used for other HNgY complexes elsewhere.^{21,23}

Three structures were found for the complex with all real vibrational frequencies, indicating that the energy minima were true (see Fig. 7). Two of the structures (complexes A and B) are linear arrangements where the Xe atom interacts with HXeBr from the H and Br ends, respectively. One structure (complex C) is bent. The interaction changes the H–Xe and Xe–Br distances with respect to the HXeBr monomer

TABLE I. Energetic and vibrational properties of the $\text{Xe}\cdots\text{HXeBr}$ complex structures. The values of the H–Xe stretching frequency and the complex interaction energy are in cm^{-1} . The interaction energy takes into account the BSSE correction and the vibrational zero-point energy.

	Monomer	Complex A	Complex B	Complex C
$\nu(\text{H-Xe})$	1792.9	1799.4	1785.3	1795.6
$E^{\text{corr}}(\text{int})$...	–261	–251	–430

where these distances are 1.7064 and 2.6878 Å, respectively. The shortest H–Xe distance is obtained for complex A and this distance is the longest for complex B. The HXeBr molecule has the shortest Xe–Br distance in complex B.

The vibrational and energetic properties of the optimized complex structures are given in Table I. The complexation increases the H–Xe stretching frequency for complexes A and C with respect to the monomer, and decreases it for complex B. The blueshift of this mode seems to be a normal case for the HNgY complexes,^{20,21} however, the redshift has been shown to be possible as well.²⁴ It is seen that the increase of the vibrational frequency correlates with shortening of the H–Xe distance, similar to the previous studies on relevant systems.^{20,21} On the other hand, we found here no clear correlation of the frequency shift with the natural charges of the atoms. Complexes A and B were found to have similar interaction energies (about -250 cm^{-1}), and complex C has larger interaction energy (-430 cm^{-1}).

B. Computational model for hindered rotation

In order to account for the two symmetrical satellite bands L_1 and L_2 in the spectra of HKrCl and HXeBr , we performed simulations of the vibrational spectra using the theory for hindered rotation originally developed by Flygare and later adapted by Apkarian and Weitz.^{25,26} In this model, only electrostatic effects on the rovibrational spectrum are considered and rotational-translational coupling effects are neglected. Furthermore, quantum effects such as Pauli repulsion due to overlapping electronic wave functions are ignored. For a fcc lattice of octahedral symmetry, Flygare showed that the first nonvanishing attractive interaction occurs between the molecular hexadecapole moment and the fourth gradient of the electric potential at the center of mass arising from the lattice atoms.

The computational procedure is the following. For a linear rotor in an octahedral crystal field, the Hamiltonian matrix is constructed using one essential parameter for the interaction strength V^J .²⁵ This parameter can be related back to the fourth gradient of the electric field arising from the lattice charges at the molecular center of mass, and it is defined as

$$V^J = \left(\frac{7}{60}\right)^{1/2} \langle l | \chi^4 | l \rangle H_d, \quad (1)$$

where χ^4 is the fourth gradient of the electric potential at the molecular center of mass, l is the electronic wave function of one atom in the noble-gas matrix, and H_d is the component of the hexadecapolar moment. The effects of centrifugal distortion have been ignored in the Hamiltonian since at low temperatures only the lowest rotational levels are populated.

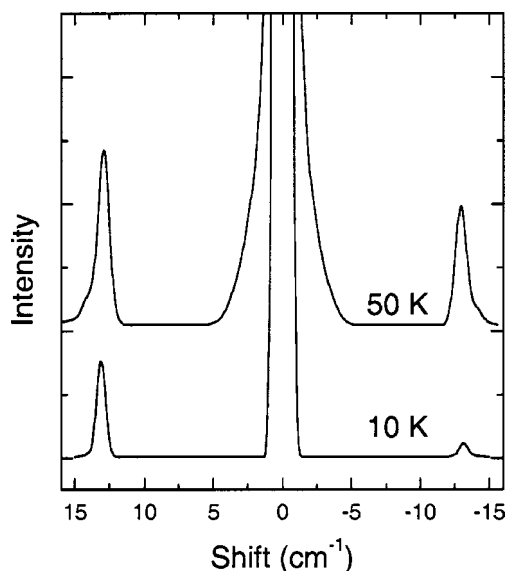


FIG. 8. Simulated librational satellites for HXeBr in a Xe matrix. The results for 10 and 50 K are shown by the lower and upper traces, respectively. The computational parameter is $V^J = 215 \text{ cm}^{-1}$.

Diagonalization of the Hamiltonian matrix gives the rotational eigenvalues and the corresponding eigenvectors of a hindered rotor in the basis of the rigid rotor basis functions. Using the obtained eigenvectors, the dipole transition moments can be calculated as

$$\langle \mu_{ij} \rangle^2 = (\langle \phi_i | D_{00}^0 | \phi_j \rangle)^2 + (\langle \phi_i | D_{01}^0 | \phi_j \rangle)^2 + (\langle \phi_i | D_{0-1}^0 | \phi_j \rangle)^2, \quad (2)$$

where D_{KM}^L are the rotational matrices and ϕ_i are the eigenvectors. When the simulated spectrum is weighted with the Boltzmann factors calculated from the energy eigenvalues, the computed spectrum can be compared with the experimental spectrum measured at the given temperature.

The spectra of HXeBr and HKrCl were simulated using a rigid rotor basis set consisting of 2601 basis functions. We tuned the interaction strength V^J until the band splitting becomes similar to the experimental value. A reasonable agreement with the experimental band splitting was obtained for $V^J = 215$ and 170 cm^{-1} for HXeBr and HKrCl, respectively. The examples of the simulated spectra are shown in Fig. 8 for the case of HXeBr and two matrix temperatures. The calculated temperature dependencies of the L_2/L_1 intensity ratios are presented in Fig. 4 for both HXeBr and HKrCl, and the agreement with the experimental data is apparently good.

IV. DISCUSSIONS

A. Matrix site structure

The structure of the main spectral feature at $1500\text{--}1503 \text{ cm}^{-1}$ (bands S_1 and S_2 , see Fig. 2) exhibits irreversible dependence on the annealing temperature and the annealing time. The lower-energy component S_2 rises faster in the early stage of annealing (35 K), and its relative contribution to the main feature monotonously decreases for longer annealing. Annealing at a higher temperature (45 K) further decreases

the S_2/S_1 intensity ratio. This behavior is a good fingerprint of the known matrix-site effect, i.e., influence of local matrix morphology on the vibrational properties of the embedded molecule. This conclusion is supported by the effect of the deposition temperature on the widths of these bands and their narrowing upon annealing at 60 K (see Fig. 5). The essential narrowing of the doublet bands suggests relaxation of the local morphology to two well-defined structures separated by an energy barrier.

The assignment of the doublet bands to the matrix sites is supported by our *ab initio* studies. The calculations show that various structures of the $\text{Xe} \cdot \cdot \text{HXeBr}$ complex can change the H–Xe stretching mode by several cm^{-1} (see Table I), which agrees with the observed S_1 – S_2 splitting of $\sim 3 \text{ cm}^{-1}$. This image is in accord with the assignment of stable and unstable configurations of HArF in solid argon to the one-to-one $\text{Ar} \cdot \cdot \text{HArF}$ complex and the uncomplexed HArF configuration done by Jolkkonen *et al.*¹⁷ The $\text{Ar} \cdot \cdot \text{HArF}$ complex shows a large computational shift of the H–Ar stretching mode in agreement with the experimental interval of $\sim 50 \text{ cm}^{-1}$ between the bands of stable and unstable HArF. This interpretation means that the interaction of HArF with one Ar matrix atom dominates in the thermally stable matrix configuration, and we call this interaction specific in contrast to interactions with other matrix atoms. In this image, the one-to-one $\text{Ar} \cdot \cdot \text{HArF}$ complex is effectively embedded in the noble-gas matrix similar to conventional matrix-isolated complexes. In the experimental consideration, the decrease of the unstable HArF bands was explained by thermal relaxation of local matrix morphology around the HArF molecule to a thermodynamically stable configuration.⁴ The influence of matrix defects and substitutional numbers on formation and thermal modification of the matrix sites is an open question.⁵

The *ab initio* energies of the $\text{Xe} \cdot \cdot \text{HXeBr}$ complexes can be used in the discussion of the actual local morphology. Complex *C* is the lowest in energy so that the strongest band at 1504 cm^{-1} is probably due to a configuration with the bent specific interaction. The weaker band S_2 may originate from uncomplexed HXeBr, i.e., from a structure without dominating interaction with a matrix atom. The assignment of the S_2 band to complex *B* is also possible even though the computational shift ($\sim 10 \text{ cm}^{-1}$) deviates more from the experiment. From the first glance, the assignment of the doublet to two complexes *A* and *C* is not supported by these computations while taking into account the annealing kinetics. Indeed, complex *A* with a higher frequency has smaller interaction energy than complex *C*, whereas in the experiments the structure with the larger frequency looks the most stable. However, this argumentation is not solid enough. First, the calculations did not take into account the deformation energy that can change the relative energies,²⁷ and this contribution can be rather large for HNgY molecules.²³ Second and more importantly, the calculations describe one-to-one complexes whereas the experiments are performed in the solid phase and the solid surrounding can modify the geometry and the relative energies. The same reason can explain why all three complex structures are not realized in the matrix. Further

consideration of this question exceeds the framework of the present work.

B. Librational band

The weak higher-energy satellites of HKrCl and HXeBr (L_1 , see Fig. 2) are connected here with hindered rotation. The important fingerprints of the librational bands are (i) the rise of a low-energy counterpart band at higher matrix temperature as computationally demonstrated in Fig. 8 and (ii) the temperature reversibility of this process. These characteristic features are observed in our experiments. The present simulations describe reasonably well the temperature dependence of the spectrum (see Fig. 4). The fact that the distance from the main spectral feature is practically the same for HKrCl and DKrCl also supports the present assignment. Indeed, the complexation-induced shifts upon deuteration are usually rather proportional to the corresponding vibrational frequency. In contrast, the librational motion depends on the moment of inertia that changes insignificantly upon deuteration of HKrCl. Recently, the blueshifted satellites have been assigned to librational motion of formic acid and CIF in an Ar matrix.^{28,29} In the previous studies the redshifted components were not demonstrated so that the present study on the HNgY molecules makes a more straightforward insight into this phenomenon.

An alternative origin of the L_1 and L_2 satellites could be interaction with lattice phonon. In general, the phonon band may appear at higher energy from the main absorption while measured at low temperatures whereas the lower-energy wing rises under increasing matrix temperature. The spectral shape should be reversible with respect to the temperature. However, this assignment is less probable compared to the libration mechanism. The phonon band should be broad and the absorption should be activated up to the Debye frequency (~ 50 and 45 cm^{-1} for solid Kr and Xe, respectively) as it was demonstrated for formic acid in low-temperature matrices.²⁸ In contrast, the L_1 and L_2 bands are quite narrow (5 – 7 cm^{-1} for HXeBr), and they are separated by ~ 15 and 20 cm^{-1} from the main spectral feature for HXeBr and HKrCl, respectively. The experimental widths are in agreement with our simulations on hindered rotation (see Fig. 8).

Many molecules of the HNgY type exhibit similar band structure with respect to the librational satellite (HXeBr, HXeI, HXeSH, HXeCN, HKrCN, HKrCl, HArF). On the other hand, some HNgY molecules (for instance, HXeCl) show no bands to be assigned to hindered rotation. Furthermore, our model does not explain why the relative intensity of the L_1 band decreases for DKrCl as compared with HKrCl. The relative intensity of the librational band shows a small change with the annealing time (see Fig. 2). The latter behavior may indicate an influence of matrix morphology on hindered rotation of the embedded molecule.

V. CONCLUDING REMARKS

We have suggested a model describing common spectral features of the H–Ng stretching mode of HNgY molecules isolated in low-temperature matrices. According to this model, the doublet of the main absorption is caused by spe-

cific interactions of the embedded molecule with noble-gas matrix atoms in certain matrix configurations (matrix-site effect). The weaker blueshifted band is probably due to hindered rotation of the HNgY molecule in the lattice. This librational band has a mirror counterpart at the low energies rising at higher matrix temperatures. The *ab initio* calculations for the one-to-one Xe $\cdot\cdot$ HXeBr complexes and simulation of hindered rotation in a matrix support this image.

The proposed model is a hypothesis and needs further theoretical support. Our *ab initio* consideration of the one-to-one Ng $\cdot\cdot$ HNgY complexes represents only an approximation for solid-state matrices, which actually often produce adequate results. The energies of various configurations of the molecules in a solid matrix need careful consideration. It should be mentioned in this respect that different computational approaches have predicted controversial energetics for HArF in solid Ar.^{16,17} The presented simulation of hindered rotation of HNgY is quite phenomenological, and it cannot give solid evidence for the hindered rotation mechanism, mostly due to the fact that all physical interactions are hidden in one adjustable parameter. A more accurate approach has been recently demonstrated by Kiljunen *et al.* for CIF in solid Ar,²⁹ however, their method needs the potentials that hinder free molecular rotation in the solid, which is a separate theoretical task for the case of HNgY molecules.

ACKNOWLEDGMENTS

The Academy of Finland supported this work. A.L. and J.J. are members of the graduate school Laskemo (Ministry of Education, Finland). E.S. thanks the University of Helsinki for the travel grant. The CSC—Center for Scientific Computing Ltd. is thanked for computer resources. Dr. Anastasia Bochenkova is thanked for providing the authors with manuscript prior to publication.

- ¹M. Pettersson, J. Lundell, and M. Räsänen, *J. Chem. Phys.* **102**, 6423 (1995).
- ²J. Lundell, L. Khriachtchev, M. Pettersson, and M. Räsänen, *Low Temp. Phys.* **26**, 680 (2000).
- ³L. Khriachtchev, M. Pettersson, N. Runeberg, J. Lundell, and M. Räsänen, *Nature (London)* **406**, 874 (2000).
- ⁴L. Khriachtchev, M. Pettersson, A. Lignell, and M. Räsänen, *J. Am. Chem. Soc.* **123**, 8610 (2001).
- ⁵L. Khriachtchev, A. Lignell, and M. Räsänen, *J. Chem. Phys.* **120**, 3353 (2004).
- ⁶L. Khriachtchev, M. Pettersson, J. Lundell, H. Tanskanen, T. Kiviniemi, N. Runeberg, and M. Räsänen, *J. Am. Chem. Soc.* **125**, 1454 (2003).
- ⁷L. Khriachtchev, H. Tanskanen, J. Lundell, M. Pettersson, H. Kiljunen, and M. Räsänen, *J. Am. Chem. Soc.* **125**, 4696 (2003).
- ⁸L. Khriachtchev, H. Tanskanen, A. Cohen, R. B. Gerber, J. Lundell, M. Pettersson, H. Kiljunen, and M. Räsänen, *J. Am. Chem. Soc.* **125**, 6876 (2003).
- ⁹V. I. Feldman, F. F. Sukhov, A. Yu. Orlov, and I. V. Tyulpina, *J. Am. Chem. Soc.* **125**, 4698 (2003).
- ¹⁰H. Tanskanen, L. Khriachtchev, J. Lundell, H. Kiljunen, and M. Räsänen, *J. Am. Chem. Soc.* **125**, 16361 (2003).
- ¹¹R. Baumfalk, N. H. Nahler, and U. Buck, *J. Chem. Phys.* **114**, 4755 (2001).
- ¹²N. H. Nahler, M. Farnik, and U. Buck, *Chem. Phys.* **301**, 173 (2004).
- ¹³M. Pettersson, J. Lundell, L. Khriachtchev, and M. Räsänen, *J. Chem. Phys.* **109**, 618 (1998).
- ¹⁴M. Pettersson, J. Lundell, L. Khriachtchev, E. Isoniemi, and M. Räsänen, *J. Am. Chem. Soc.* **120**, 7979 (1998).
- ¹⁵M. Pettersson, L. Khriachtchev, A. Lignell, M. Räsänen, Z. Bihary, and R. B. Gerber, *J. Chem. Phys.* **116**, 2508 (2002).

- ¹⁶Z. Bihary, G. M. Chaban, and R. B. Gerber, *J. Chem. Phys.* **116**, 5521 (2002).
- ¹⁷S. Jolkkonen, M. Pettersson, and J. Lundell, *J. Chem. Phys.* **119**, 7356 (2003).
- ¹⁸A. V. Bochenkova, D. A. Firsov, and A. V. Nemukhin, *Chem. Phys. Lett.* (to be published).
- ¹⁹V. I. Feldman and F. F. Sukhov, *Chem. Phys. Lett.* **255**, 425 (1996).
- ²⁰A. V. Nemukhin, B. L. Grigorenko, L. Khriachtchev, H. Tanskanen, M. Pettersson, and M. Räsänen, *J. Am. Chem. Soc.* **124**, 10706 (2002).
- ²¹A. Lignell, L. Khriachtchev, M. Pettersson, and M. Räsänen, *J. Chem. Phys.* **118**, 11120 (2003).
- ²²M. J. Frisch, G. W. Trucks, H. B. Schlegel *et al.*, GAUSSIAN03, Revision B.02 Gaussian, Inc., Pittsburgh, PA, 2003.
- ²³A. Lignell, L. Khriachtchev, M. Pettersson, and M. Räsänen, *Chem. Phys. Lett.* **390**, 256 (2004).
- ²⁴S. A. C. McDowell, *Phys. Chem. Chem. Phys.* **5**, 808 (2003).
- ²⁵H. Flygare, *J. Chem. Phys.* **39**, 2263 (1963).
- ²⁶V. A. Apkarian and E. Weitz, *J. Chem. Phys.* **76**, 5796 (1982).
- ²⁷F. B. van Duijneveldt, J. G. C. M. van Duijneveldt-van de Rijdt, and J. H. van Lenthe, *Chem. Rev. (Washington, D.C.)* **94**, 1873 (1994).
- ²⁸E. M. S. Maçôas, L. Khriachtchev, M. Pettersson, J. Juselius, R. Fausto, and M. Räsänen, *J. Chem. Phys.* **119**, 11765 (2003).
- ²⁹T. Kiljunen, M. Bargheer, M. Guehr, N. Schwentner, and B. Schmidt, *Phys. Chem. Chem. Phys.* **6**, 2932 (2004).
- ³⁰L. Khriachtchev, M. Saarelainen, M. Pettersson, and M. Räsänen, *J. Chem. Phys.* **118**, 6403 (2003).